HHS Public Access

Author manuscript

J Hepatol. Author manuscript; available in PMC 2018 August 01.

Published in final edited form as:

J Hepatol. 2017 August ; 67(2): 246–254. doi:10.1016/j.jhep.2017.03.027.

Selection of the highly replicative and partially multidrug resistant rtS78T HBV polymerase mutation during TDF-ETV combination therapy

Elham Shirvani-Dastgerdi[1,2], **Benjamin Y. Winer**[2], **Toni Celià-Terrassa**[2], **Yibin Kang**[2], **David Tabernero**[3,4], **Eray Yagmur**[5], **Francisco Rodríguez-Frías**[3,4], **Josep Gregori**[6], **Tom Luedde**[1], **Christian Trautwein**[1], **Alexander Ploss**[2], and **Frank Tacke**[1]

[1]Department of Medicine III, RWTH-University Hospital Aachen, Aachen, Germany

[2]Department of Molecular Biology, Princeton University, Princeton, NJ, USA

[3]Centro de Investigación Biomédica en Red de Enfermedades Hepáticas y Digestivas (CIBERehd), Instituto de Salud Carlos III, Madrid, Spain

[4]Liver Unit, Vall d'Hebron Institute of Research (VHIR), Universitat Autònoma de Barcelona (UAB), Barcelona, Spain

[5]Medical Care Centre, Dr Stein and Colleagues, Mönchengladbach, Germany

[6]Roche Diagnostics SL, Sant Cugat del Vallès, Spain

Abstract

Background & Aims—Patients chronically infected with the hepatitis B virus (HBV) that are on long-term treatment with nucleoside or nucleotide analogues are at risk of selecting HBV strains with complex mutational patterns. We herein report two cases of HBV-infected patients with insufficient viral suppression despite dual antiviral therapy with entecavir (ETV) and tenofovir (TDF), of which one patient died from aggressive hepatocellular carcinoma (HCC).

Methods—Serum samples of the patients from different time-points were analyzed by ultra-deep pyrosequencing analysis. Identified HBV mutations were functionally analyzed after transient transfection of replication-competent HBV vectors into hepatoma cells *in vitro*. We assessed replication efficacy, resistance to antivirals and potential impact on HBV secretion (viral particles, exosomes).

Results—Sequencing analyses revealed the selection of the rtS78T HBV polymerase mutation in both cases that simultaneously creates a premature stop codon at sC69 and thereby deletes almost the entire small HBV surface protein. One of the patients had an additional 261-bp deletion in the

Corresponding author: Frank Tacke, MD, PhD, Department of Medicine III, RWTH-University Hospital Aachen, Aachen, Germany. frank.tacke@gmx.net.

Author names in **bold** designate shared co-first authorship.

Conflict of interest: Dr. Josep Gregori is an employee of Roche Diagnostics. The other authors declare no conflict of interest.

Authors' contributions: ES: conduction of experiments, analysis and interpretation of data; drafting of the manuscript. BYW, ACT, YK: conducted *in vitro* experiments and provided exosome analyses. DT, FRF, JG: performed ultra deep sequencing and analysed results. EY, TL, CT, AP: provided important methodological tools, critical revision of the manuscript, important intellectual content. FT: study concept and design; study supervision; drafting of the manuscript. All authors have read and approved the manuscript.

preS1/S2 region. Functional analyses of the mutations *in vitro* revealed that the rtS78T/sC69* mutation, but not the preS1/S2 deletion, significantly enhanced viral replication and conferred reduced susceptibility to ETV and TDF. The sC69* mutation caused truncation of HBs protein, leading to impaired detection by commercial HBsAg assay, without causing intracellular HBsAg retention or affecting HBV secretion.

Conclusions—The rtS78T/c69* HBV mutation associated with enhanced replication and insufficient response to antiviral treatment may favor long-term persistence of these isolates. Along with increased production of HBV transcripts and the sustained secretion of viral particles in the absence of antigenic domains of S protein, this HBV mutation may predispose to carcinogenic effects.

Graphical abstract

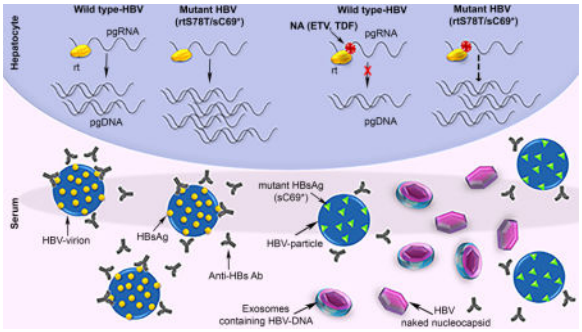

Keywords

HBV; drug resistance; HCC; mutations; HBsAg; exosome

Introduction

Over 240 million people are chronically infected with the hepatitis B virus (HBV) worldwide. Despite advances in vaccination and treatment, HBV-related deaths due to liver cirrhosis or hepatocellular carcinoma (HCC) have increased between 1990 and 2013 globally by 33% to >686,000 cases in 2013 [1]. Therefore, the main treatment goal for chronic hepatitis B is to suppress viral replication and consequently to prevent progression of the disease [2]. In most cases, this is achieved by the orally available nucleos(t)ide analogues that act as competitive inhibitors of the HBV reverse transcriptase, as their incorporation into the DNA strand provokes chain termination and hence suppresses HBV replication. One of the major problems with using nucleos(t)ide analogues has been the development of drug resistance mutations during long term therapy [3]. Factors that determine the risk of selecting antiviral therapy-resistant mutants include pre-treatment HBV DNA level, the choice of the antiviral (with a low/high barrier to resistance), the duration of treatment, the on-treatment response to antivirals as well as prior exposure to nucleos(t)ide analogues [3].

In order to reduce the risk of drug resistance, all guidelines now recommend the use of highly potent antivirals with a high barrier to resistance such as entecavir (ETV) or tenofovir

(TDF) [4]. If ETV is used as first-line therapy (without prior lamivudine (LAM) exposure), the rate of resistance is very low, approximately 1% or less after 5 years of therapy [5]. The molecular explanation is that ETV resistance usually requires the LAM-resistant "YMDD mutation(s)" (rtM204V/I ±L180M) plus an additional ETV 'signature' substitution in the B domain (rtI169T or rtS184G), C domain (rtS202G/I), or E domain (rtM250V) [3]. Moreover, these ETV-resistance mutations in the HBV genome drastically reduce viral replication when compared to wildtype HBV *in vitro* [6]. In case of TDF, no signature mutation for TDF resistance has been identified in prospective patient cohorts to date even after seven years of therapy [7], although cases of insufficient responses to TDF have been reported [8,9]. Notably, mutations in the HBV polymerase-open reading frame (P-ORF) related to drug resistance may alter the amino acid sequence of the surface antigen proteins (S), because of the overlapping reading frames of the P and S gene [10].

We herein report two patient cases with insufficient responses to dual TDF and ETV treatment. Molecular analyses revealed the presence of the rtS78T mutation that created a stop codon (sC69*) for HBsAg. Functional analyses indicated that this mutation affect viral replication and susceptibility to ETV/TDF, thereby providing novel molecular insights into high-risk mutational patterns of HBV during long-term antiviral treatment.

Materials & Methods

Patient samples and sequencing

We identified the two HBV-infected patients with insufficient response to antiviral therapy from our outpatient clinic (University Hospital Aachen, Germany). Serum samples from two time-points each were subjected to ultra-deep pyrosequencing [11] and direct PCR analyses. Information regarding the primer sequences can be found in the Supplementary CTAT Table.

Plasmid construction and *in vitro* analyses

To investigate the effects of rtS78T/sC69* and preS1/preS2del mutations on replication of HBV, three replication-competent HBV constructs containing the rtS78T/sC69* mutation (M1), the preS1/S2 deletion (preS1/preS2del, M2) with an in frame deletion of the nucleotides 1124 to 1385 as well as the combination of the two, rtS78T/sC69* + preS1/S2del (M3), were generated using site directed mutagenesis and recombination techniques [12]. Human hepatoma Huh7 cells were transiently transfected with the replication-competent HBV plasmid constructs, as described previously [13]. Hepatitis B surface antigen (HBsAg) and HBeAg were measured in the supernatant by commercially available kits (Modular Analytics E170, Roche Diagnostics, Mannheim, Germany). The values were normalized to the beta-Gal transfection efficiency.

HBV-DNA isolation and qPCR

HBV progeny DNA from transfected cells and HBV-DNA from secreted particles were isolated and analyzed to evaluate viral replication, as previously described [12–14]. In brief, cells were lysed seven days after transfection. HBV-capsids were then immunoprecipitated by polyclonal rabbit anti-hepatitis B core antibody (Dako, Carpinteria, CA, USA) and protein-A agarose beads (Roche). HBV progeny DNA was extracted subsequently through

alcohol precipitation. To isolate HBV DNA from secreted particles, three different approaches were applied: (a) polyethylene glycol precipitation (PEG, Sigma, St. Louis, MO, USA), followed by capsid digestion and alcohol precipitation of DNA; (b) immune precipitation of released particles by using preS1 (Santa Cruz Biotechnology, USA) and core (Thermo Fisher, USA) antibodies and isolation of the DNA (QIAamp DNA mini kit, Qiagen, USA); (c) ultra-centrifugation of the supernatants (110,000x g, 70 min) [15], evaluation of the concentration of pelleted particles using the LM10 nanoparticle characterization system in real-time (NanoSight, Malvern Instruments) equipped with a blue laser (405 nm) followed by isolation of exosomes from precipitated particles by using an Exosome-Human CD63 isolation/detection reagent (Thermo Fisher) and extraction of DNA (QIAamp DNA mini kit). A 5 μl aliquot of HBV DNA isolated from immunoprecipitated particles (using preS1 and core antibodies) and exosomes was subjected per reaction well to qPCR analysis, using the iTaq Universal SYBR Green One-Step qPCR kit (BioRad, Hercules, CA). The information about primer and probe sequences are provided in the Supplementary CTAT Table.

Southern blot analysis of HBV DNA

Isolated DNAs from cells (through immunoprecipitation of the capsids) and supernatants (through PEG precipitation) were transferred to positively charged nylon membranes (Roche) after running on 1% agarose gel via capillary transfer method and subsequently detected using random primed DIG-labeled HBV DNA probe (DIG High Prime DNA labeling and detection starter kit II, Roche). Data were quantified by ImageJ software and normalized to total protein content of the cell lysate (for progeny DNA only) and beta-Gal transfection efficiency (for both).

HBV-RNA extraction and northern blot analysis

Total RNA was isolated from Huh7 cells three days after transfection with the RNeasy kit (Qiagen). RNA samples were run on a 1.2% formaldehyde gel, transferred to a nylon membrane via capillary transfer method and labeled with a full-length DIG-labeled HBV-DNA (Roche). Quantification of data was done with ImageJ software, and results were normalized to ribosomal RNA (rRNA) content of the cell lysate (for cellular RNA) and beta-Gal transfection efficiency.

Flow cytometry analysis

Huh7 cells were collected 6 days post transfection and fixed with fixation buffer (1% FBS, 4% PFA in PBS) followed by staining with anti-pre-S1 (Santa Cruz, Dallas, Texas, USA), -pre-S2 and –core (Thermo Fisher) as primary antibodies and goat anti-mouse Alexa Fluor 647 (Thermo Fisher) as the secondary antibody. Flow cytometry analysis was performed using an LSRII Flow Cytometer (BD Biosciences). Data were analyzed using FlowJo software.

Antiviral compounds and drug susceptibility analysis

ETV was purchased from Moravek Biochemicals, Brea, CA, USA, and TDF was provided by Gilead Sciences, Foster City, CA. To calculate the susceptibility of HBV to antiviral

drugs, Huh7 cells transfected with HBV constructs were cultured in the presence of different concentrations of ETV or TDF, followed by southern blot assay of extracted HBV progeny DNA. Southern blot assay results were normalized to the total protein content of the cell lysate and transfection efficiency based on beta-galactosidase activity. The concentration of the antiviral component resulting in the inhibition of HBV replication by 50% was considered the 50% effective concentration (EC50) [16].

Statistics

Statistical analyses of experimental data were conducted using GraphPad Prism (GraphPad Software, San Diego California USA). Experimental results are reported as mean ± standard deviation. One-way ANOVA with Bonferroni post-test was applied for comparisons between the groups; a P-value of <0.05 was considered statistically significant.

Results

Two patients with insufficient response to antiviral therapy

Patient A—A 53-year-old Caucasian man with chronic HBeAg negative HBV infection presented to our outpatient clinic in August 2009 with a baseline HBV viral load of 6×10^5 copies/ml (Fig. 1A, left panel). During the initial work-up, liver biopsy revealed grade 2 inflammation and stage 1 fibrosis, but simultaneously a 3.4 cm hepatic nodule in segment IV suspicious of HCC. The HCC was histologically confirmed and resected completely (R0). TDF therapy was started immediately, which resulted in reduction of HBV DNA to undetectable levels (<34 copies/ml) by qPCR analysis for 21 months. The patient was regularly (3-6 months) followed for HBV suppression and HCC surveillance. About 2.5 years later (March 2012), HBV viral load increased (Fig. 1A, left panel) without detection of HCC nodules at that time. ETV was added to TDF, but was insufficient in suppressing HBV replication. About three months later (June 2012), recurrent HCC was diagnosed, resulting in hemihepatectomy of the right liver lobe. Unfortunately, HCC was multifocal upon histological processing with invasion of blood vessels and portal vein thrombosis. Notably, non-tumorous liver tissue revealed no cirrhosis (inflammation grade 1, fibrosis stage 1-2). Due to another HCC recurrence, sorafenib was started in March 2013, but the patient passed away of advanced tumor disease in April 2013. HBV DNA remained positive at low levels during ETV/TDF combination therapy (Fig. 1A, left panel). Serum samples of the patient were collected and analysed at two time points after increase of HBV viral load during TDF therapy (30 and 37 months after initiation of TDF).

Patient B—A 41-year-old Asian woman with chronic HBeAg positive HBV infection and a high viral load (baseline $2x10^9$ copies/ml) presented to our outpatient clinic in January 2008. Liver biopsy revealed moderate signs of inflammation (grade 1-2) and early fibrosis (stage 1), while ALT levels were repeatedly measured above the upper limit of normal (Fig. 1A, right panel). Thus, the patient was started with ETV. Notably, viral load only slowly declined during ETV therapy (e.g., 850 copies/ml at 18 months after treatment). In November 2009, an increase in viral load by about 1-log was noted, which prompted the addition of TDF to the ETV therapy. However, even dual antiviral therapy never fully suppressed HBV DNA levels in this patient (Fig. 1A, right panel). This patient did not

display evidence for HCC on regular follow-up by ultrasound. Serum samples were collected and analysed at months 48 and 57 after ETV treatment. In 2013, the patient stopped both drugs at her own decision. Her viral loads remain high due to cessation of treatment.

Selection of the rtS78T and sC69* mutations during dual antiviral treatment

For both cases, serum samples from two time-points each were subjected to ultra-deep pyrosequencing (UDPS) analyses. Our UDPS analysis revealed over-representation of the rtS78T mutation in the reverse transcriptase (rt) gene of the HBV genome that creates a premature stop codon in the overlapping surface (s) protein at sC69, thereby deleting almost the entire small HBV surface protein [17]. In patient A (Fig. 1A, left panel), 93.05% of the viral population were detected with rtS78T and 93.22% with sC69* (* represents the stop codon) at first analysis, and at the second sampling (6 months later), the entire isolates were carrying rtS78T/sC69* mutations. Patient B showed 13.96% frequency for rtS78T and 14.21% for sC69* at first sampling, which increased to 38.16% for rtS78T and 37.78% for sC69* 8 months later (Fig. 1A, right panel and Table 1).

By linkage analysis, the stop codon in the S-open reading frame (S-ORF) was always linked to sI68T, which is a silent mutation in polymerase-ORF (Table 1). While sC69* is invariably linked to sI68T, rtS78T seems to occur preferentially alone, and only in very low percentages with other variants. Other mutations, especially those related to LAM or ETV resistance (rtL180M and rtM204V/I) and classical immune escape (sG145R and/or P120T) variants were noted at no or very low frequencies (Table 1), despite ETV treatment [10].

Moreover, direct sequencing also revealed a 261 in-frame nucleotide deletion (nt 1124 to 1385) at the preS1/preS2 junction in patient B at both time points. The relative position of the observed mutations in the two patients to the coding regions in the HBV genome, including preS1/S2 deletion and rtS78T/sC69*, is shown in Fig. 1B. The 261 preS1/preS2 nucleotide deletion of patient B is shown in alignment with a genotype A wild type HBV (Genebank accession number: AY741797; Fig. 1C).

Functional consequences of rtS78T/sC69* and preS1/preS2del on viral replication and secretion

To investigate the effects of rtS78T/sC69* and preS1/preS2del mutations on replication of HBV, three replication-competent HBV constructs containing the rtS78T/sC69* mutation (M1), the preS1/S2 deletion (preS1/preS2del, M2) as well as the combination of the two, rtS78T/sC69* + preS1/S2del (M3), were generated and studied using transient transfection of Huh7 human hepatoma cells. As anticipated from the sC69* stop mutation, no HBsAg was detectable using anti-HBs antibodies (Fig. 2A), whereas the expression of HBeAg was not impaired by the mutations. The preS1/preS2del mutation is not expected to diminish secretion or detection of the S protein. However, we were not able to detect HBsAg in the supernatant of M2 transfected cells (Fig. 2A). This effect has been reported earlier for some other preS1 mutations related to occult HBV phenotype, too [18]. While the transcriptional expression of S-mRNA was not abolished by the mutants, the level of 3.5-kb HBV-transcripts (pregenomic / pgRNA and precore-RNA) in M1 and M3 experiments was

significantly higher compared to wild type HBV (Fig. 2B). The preS1/preS2del variant (M2) displayed reduced pgRNA levels compared to wild type. Co-transfection of wild type construct with the mutants resulted in restoration of pgRNA for the M2 to that of wild type level, but did not change the pgRNA levels for M1 and M3 (Fig. 2C).

To investigate if the presence of rtS78T/sC69* has a general impact on cellular transcription level ("transactivator function"), we performed a co-transfection of wild type and mutant HBV constructs with pCDNA3.1(-)-eGFP. Our results suggest that wild type HBV can support and elevate GFP gene expression in trans (Fig. 2D), as also reported previously [19]. The rtS78T/sC69* caused the same increase in GFP expression and interestingly could also restore the neutral effect of preS1/preS2del (M2) on GFP expression, presumably through an increase in viral replication and hence the expression of X protein (Fig. 2D).

To further investigate the potential impact of rtS78T/sC69* and preS1/preS2del mutations on virion release, when S protein is defective or absent, we performed HBV-DNA analysis on the isolated exosomes from supernatants as well as immunoprecipitated viral particles by using mouse monoclonal preS1 and core antibodies. Based on the known role of exosomes in HBV release and transmission, we pelleted the released particles from hepatocytes through ultracentrifugation and washing steps, monitored the particles and measured their concentrations through nanoparticle tracking analysis (Fig. 3A, 3D-plots and concentration table). Following extraction of DNA from isolated exosomes and qPCR analysis, we detected exosome-mediated secretion of HBV-DNA in all HBV transfected samples (Fig. 3B). Moreover, the premature stop codon at S (M1) did not reduce the secreted HBV-DNA level associated with anti-preS1 isolated particles. Deletion at preS1/preS2del (M2, M3), however, caused a significant reduction in released HBV-DNA compared to wild type HBV (Fig. 3C). Our findings also indicated virion release through naked nucleocapsids for both wild type and mutant HBV isolates (Fig. 3D). The relevant position of sC69* and preS1/preS2 mutations in multispanning transmembrane surface proteins of HBV is schematically shown in Fig. 3E. As our data suggest, these mutations may not completely hinder the process of nucleocapsid envelopment for the studied mutations.

To assess whether these mutations have any impact on the S and core protein expression levels within the cell, we harvested the cells 6 days post transfection and performed flow cytometry analysis on the samples by using relevant antibody complexes. Reduced expression levels of HBsAg because of mutations in the surface protein coding region have been reported previously [20,21]. Accordingly, all three sets of mutations resulted in a significant decrease in surface protein levels (Fig. 4), demonstrating no intracellular retention of (truncated) S-proteins related to the mutants. However, the core protein expression was increased due to the rts78T/sC69* mutation in M1, compared to the wild type HBV (Fig. 4).

Susceptibility of the mutants to antiviral drugs

We next measured the intracellular HBV-DNA and HBV-progeny DNA levels (indicating active replication) to evaluate the effects of the respective mutations on viral replication. All three variants (M1-M3) significantly increased the replication capacity, by increasing the progeny DNA levels up to 1.5-fold compared to wildtype virus during six days of transient

transfection in hepatoma cells (Fig. 5A). The extracellular HBV-DNA followed the same trend as the intracellular progeny DNA (Fig. 5B), indicating that, despite the truncated HBsAg, virion secretion is not impaired due to these mutations.

Based on the emergence of rtS78T/sC69* and preS1/preS2deldeletion during dual ETV/TDF therapy in patients, we next assessed the susceptibility of the mutants to ETV or TDF *in vitro* by measuring the intracellular HBV-DNA and HBV-progeny DNA levels (indicating active replication) and also the extracellular HBV-DNA that was extracted from PEG precipitated particles. ETV (1 μM) or TDF (20 μM) exposure was associated with a >50% reduction in intracellular HBV DNA formation in wild type virus, while M1 and M3 (both containing the rtS78T mutation) retained a higher replication level (Fig. 5A). The extracellular HBV-DNA followed the same trend as the intracellular progeny DNA (Fig. 5B), again indicating that despite of vastly truncated S protein, HBV-DNA secretion is not impaired.

More detailed analysis on the resistance level of the mutants revealed 1.57- and 1.63-fold changes in the half maximal effective concentration (EC50) to ETV and TDF treatment (compared to the wild type HBV) related to rtS78T/sC69* in M1 and M3 mutants (Fig. 5C), indicating decreased susceptibility to antivirals. The preS1/S2 deletion (in M2) was not associated with altered susceptibility to antiviral treatments (EC50 1.1 and 1.23 to ETV and TDF, Fig. 5C).

Discussion

In this study, we describe the development of the rtS78T/sC69* mutation during long-term antiviral therapy in two patients with chronic HBV infection. In patient A, this mutation presumably developed during TDF monotherapy, was further selected during TDF/ETV combination therapy, and was associated with aggressive and ultimately fatal HCC. In patient B, this mutation arose during ETV/TDF combination therapy and was additionally accompanied by a 261 in-frame nucleotide deletion in the preS1/S2 region. Our *in vitro* analyses indicated an enhanced replicative efficacy for rtS78T/sC69* as well as a partial resistance to ETV and to TDF.

Selection of HBV isolates with truncated S proteins has been reported during nucleos(t)ide analogue treatment and may contribute to HCC development [22–24]. In this regard, the emergence of rtS78T/sC69* mutation has been occasionally reported in the literature [21,22,25]. The presence of rtS78T in addition to rtT184S, rtV173L, rtL180M, and rtM204V, was associated with a two-fold reduction in ETV susceptibility; however, in line with our results, the ETV resistance level for this mutation alone did not exceed 1.8-fold of the level of wild type HBV [26–29]. Furthermore, the rtS78T exchange was also found to be increased in adefovir-treated patients suggesting a potential resistance to adefovir alone or in combination with other resistance mutations [17]. Moreover, based on computational studies rtS78T mutation implies a large affinity loss for TDF [30].

One possibility for the observed level of partial multidrug resistance related to this mutation might be the proximity of S78 to the residue D83, which along with YMDD forms the

catalytic centre of the reverse transcriptase [17]. In this regard, the rtL80I was shown to be associated with restoring viral replication and increasing drug resistance properties of LAM-resistant isolates with impaired replication [31]. However, we did not observe associated rtL80I substitutions by sequencing in our cases.

The HBV genome contains four promoters that control transcription of five major viral RNAs. These include precore promoter (PC), preS1, preS2 and X promoters. The PC promoter controls the largest HBV transcript (pgRNA, 3.5Kb), which encodes the HBV polymerase, the cellular core protein (HBcAg) and its secretory form (HBeAg). The pgRNA also serves as the template for RT to generate pgDNA [10]. The increased 3.5Kb HBV-RNA, pgDNA and HBeAg levels due to rtS78T and to a lesser extent preS1/S2del mutations, could possibly indicate a cis-acting role exerted by this domain of the viral genome to up-regulate transcription from PC. This is very similar to the role of the HBV-enhancer element I (EnhI) in stimulation and up-regulation of PC and HBx-mRNAs [32]. However, these mutations are located 752 (rtS78T) and 1104 (preS1/S2del) nucleotides upstream of the known EnhI. Whether this domain of HBV genome has similar properties as Enh elements in controlling PC or other HBV promoters or if these mutations result in elevation of HBV-polymerase activity need further investigations.

It has been speculated that truncated S proteins, like those having sC69*, may result in secretion incompetent variants due to the deletion of the HBsAg C-terminal domain [21,23]. However, in our study, we could detect HBV-DNA in the supernatant of transfected hepatocytes through PEG precipitation and preS1 or core immunoprecipitation, in secreted particles as well as in exosomes.

In a recent study, Xiang et. al, have reported on the effects of S mutations on HBV replication and release. They showed that truncated S proteins with sC69* are only detectable intracellularly and through an HA Tag domain fused with HBs [21]. The negative results for the detection of secreted envelop proteins in this study might be due to the internal positioning of the S N-terminal domain (and HA Tag) in secreted particles, which make the epitopes inaccessible to the antibodies. They also reported a significant reduction in HBV genome levels, (DNA and RNA) both intra and extracellularly, under the influence of sC69*. These differences in observations might be due to the different HBV genotypes being used by the two studies (genotype A in our study vs. genotype C) or the applied methodology to detect HBV DNA and RNA (Southern and Northern blots vs. qPCR analysis).

According to the literature, the N terminal part of preS1 is responsible for receptor binding and host tropism, and the C terminal domain of preS1 and N terminal region of preS2 are involved in HBV nucleocapsid envelopment [33]. Therefore, as also observed in the second serum analysis of patient A with detectable serum HBV-DNA in spite of 100% frequency of sC69*, a stop codon at S may not hinder the entire process of particle envelopment and release for mutated variants but possibly the stability of secreted virions. Indeed, the Cys residues within the S domain form several disulfide bonds that confer stability to the virions and might also be essential for the virion uptake and productive infection [34]. Although we did not examine the infectious ability of the isolates with sC69*, infection of new

hepatocytes through alternative secretion of the isolates, as evidenced via exosomes in our study, is expected even if the incomplete structure of envelop proteins does not support the infectivity [15].

In conclusion, we herein show the selection of functionally relevant rtS78T/sC69* mutation in two HBV-infected patients with TDF/ETV combination therapy. The *in vitro* functional analyses of this mutation revealed a higher replication competence associated with reduced susceptibility to ETV and TDF. We could also determine virion release in the absence of detectable S protein that in turn hides the virus from being recognized by neutralizing antibodies, thereby representing occult HBV phenotypes. The immune response evasion of this mutant and its persistence during antiviral therapy is an indication for its particular risk of selecting during long-term antiviral therapy and the subsequent complications including developing hepatocellular carcinoma.

Acknowledgments

This work was supported in part by the German Research Foundation (SFB/TRR57, Ta434/3-1), the IZKF Aachen (E7-1), and the European Regional Development Fund (ERDF, PI15/00856). B.Y.W. is a recipient of the F31 Ruth L. Kirschstein Fellowship from the NIAID. E.S.D. is a recipient of a postdoctoral fellowship from the German Research Foundation (DFG, 1085/1-1), and A.C.T. has received a fellowship from New Jersey Commission on Cancer Research (NJCC).

References

1. Stanaway JD, Flaxman AD, Naghavi M, Fitzmaurice C, Vos T, Abubakar I, Abu-Raddad LJ, Assadi R, Bhala N, Cowie B, et al. The global burden of viral hepatitis from 1990 to 2013: findings from the Global Burden of Disease Study 2013. Lancet. 2016
2. European Association For The Study Of The L. EASL clinical practice guidelines: Management of chronic hepatitis B virus infection. J Hepatol. 2012; 57:167–185. [PubMed: 22436845]
3. Zoulim F, Locarnini S. Optimal management of chronic hepatitis B patients with treatment failure and antiviral drug resistance. Liver Int. 2013; 33(Suppl 1):116–124. [PubMed: 23286855]
4. Terrault NA, Bzowej NH, Chang KM, Hwang JP, Jonas MM, Murad MH, American Association for the Study of Liver D. AASLD guidelines for treatment of chronic hepatitis B. Hepatology. 2016; 63:261–283. [PubMed: 26566064]
5. Chang TT, Lai CL, Kew Yoon S, Lee SS, Coelho HS, Carrilho FJ, Poordad F, Halota W, Horsmans Y, Tsai N, et al. Entecavir treatment for up to 5 years in patients with hepatitis B e antigen-positive chronic hepatitis B. Hepatology. 2010; 51:422–430. [PubMed: 20049753]
6. Amini-Bavil-Olyaee S, Herbers U, Luedde T, Trautwein C, Tacke F. Impact of hepatitis B e antigen-suppressing mutations on the replication efficiency of entecavir-resistant hepatitis B virus strains. J Viral Hepat. 2011; 18:804–814. [PubMed: 20887378]
7. Buti M, Tsai N, Petersen J, Flisiak R, Gurel S, Krastev Z, Schall RA, Flaherty JF, Martins EB, Charuworn P, et al. Seven-year efficacy and safety of treatment with tenofovir disoproxil fumarate for chronic hepatitis B virus infection. Dig Dis Sci. 2015; 60:1457–1464. [PubMed: 25532501]
8. Sheldon J, Camino N, Rodes B, Bartholomeusz A, Kuiper M, Tacke F, Nunez M, Mauss S, Lutz T, Klausen G, et al. Selection of hepatitis B virus polymerase mutations in HIV-coinfected patients treated with tenofovir. Antivir Ther. 2005; 10:727–734. [PubMed: 16218172]
9. Amini-Bavil-Olyaee S, Herbers U, Sheldon J, Luedde T, Trautwein C, Tacke F. The rtA194T polymerase mutation impacts viral replication and susceptibility to tenofovir in hepatitis B e antigen-positive and hepatitis B e antigen-negative hepatitis B virus strains. Hepatology. 2009; 49:1158–1165. [PubMed: 19263474]
10. Tong S, Revill P. Overview of hepatitis B viral replication and genetic variability. J Hepatol. 2016; 64:S4–16. [PubMed: 27084035]

11. Margeridon-Thermet S, Shulman NS, Ahmed A, Shahriar R, Liu T, Wang C, Holmes SP, Babrzadeh F, Gharizadeh B, Hanczaruk B, et al. Ultra-deep pyrosequencing of hepatitis B virus quasispecies from nucleoside and nucleotide reverse-transcriptase inhibitor (NRTI)-treated patients and NRTI-naive patients. J Infect Dis. 2009; 199:1275–1285. [PubMed: 19301976]
12. Amini-Bavil-Olyaee S, Herbers U, Mohebbi SR, Sabahi F, Zali MR, Luedde T, Trautwein C, Tacke F. Prevalence, viral replication efficiency and antiviral drug susceptibility of rtQ215 polymerase mutations within the hepatitis B virus genome. J Hepatol. 2009; 51:647–654. [PubMed: 19586679]
13. Shirvani-Dastgerdi E, Pourkarim MR, Herbers U, Amini-Bavil-Olyaee S, Yagmur E, Alavian SM, Trautwein C, Tacke F. Hepatitis delta virus facilitates the selection of hepatitis B virus mutants in vivo and functionally impacts on their replicative capacity in vitro. Clin Microbiol Infect. 2016; 22:98e91–96.
14. Tacke F, Gehrke C, Luedde T, Heim A, Manns MP, Trautwein C. Basal core promoter and precore mutations in the hepatitis B virus genome enhance replication efficacy of Lamivudine-resistant mutants. J Virol. 2004; 78:8524–8535. [PubMed: 15280461]
15. Yang Y, Han Q, Hou Z, Zhang C, Tian Z, Zhang J. Exosomes mediate hepatitis B virus (HBV) transmission and NK-cell dysfunction. Cell Mol Immunol. 2016
16. Amini-Bavil-Olyaee S, Vucur M, Luedde T, Trautwein C, Tacke F. Differential impact of immune escape mutations G145R and P120T on the replication of lamivudine-resistant hepatitis B virus e antigen-positive and -negative strains. J Virol. 2010; 84:1026–1033. [PubMed: 19889778]
17. Cento V, Van Hemert F, Neumann-Fraune M, Mirabelli C, Di Maio VC, Salpini R, Bertoli A, Micheli V, Gubertini G, Romano S, et al. Anti-HBV treatment induces novel reverse transcriptase mutations with reflective effect on HBV S antigen. J Infect. 2013; 67:303–312. [PubMed: 23796863]
18. Kim H, Lee SA, Kim DW, Lee SH, Kim BJ. Naturally occurring mutations in large surface genes related to occult infection of hepatitis B virus genotype C. PLoS One. 2013; 8:e54486. [PubMed: 23349904]
19. van Breugel PC, Robert EI, Mueller H, Decorsiere A, Zoulim F, Hantz O, Strubin M. Hepatitis B virus X protein stimulates gene expression selectively from extrachromosomal DNA templates. Hepatology. 2012; 56:2116–2124. [PubMed: 22744635]
20. Chen J, Liu Y, Zhao J, Xu Z, Chen R, Si L, Lu S, Li X, Wang S, Zhang K, et al. Characterization of Novel Hepatitis B Virus PreS/S-Gene Mutations in a Patient with Occult Hepatitis B Virus Infection. PLoS One. 2016; 11:e0155654. [PubMed: 27182775]
21. Xiang KH, Michailidis E, Ding H, Peng YQ, Su MZ, Li Y, Liu XE, Dao Thi VL, Wu XF, Schneider WM, et al. Effects of amino acid substitutions in hepatitis B virus surface protein on virion secretion, antigenicity, HBsAg and viral DNA. J Hepatol. 2017; 66:288–296. [PubMed: 27650283]
22. Betz-Stablein BD, Topfer A, Littlejohn M, Yuen L, Colledge D, Sozzi V, Angus P, Thompson A, Revill P, Beerenwinkel N, et al. Single-Molecule Sequencing Reveals Complex Genome Variation of Hepatitis B Virus during 15 Years of Chronic Infection following Liver Transplantation. J Virol. 2016; 90:7171–7183. [PubMed: 27252524]
23. Warner N, Locarnini S. The antiviral drug selected hepatitis B virus rtA181T/sW172* mutant has a dominant negative secretion defect and alters the typical profile of viral rebound. Hepatology. 2008; 48:88–98. [PubMed: 18537180]
24. Shirvani-Dastgerdi E, Schwartz RE, Ploss A. Hepatocarcinogenesis associated with hepatitis B, delta and C viruses. Curr Opin Virol. 2016; 20:1–10. [PubMed: 27504999]
25. Huang SF, Chen YT, Lee WC, Chang IC, Chiu YT, Chang Y, Tu HC, Yuh CH, Matsuura I, Shih LY, et al. Identification of transforming hepatitis B virus S gene nonsense mutations derived from freely replicative viruses in hepatocellular carcinoma. PLoS One. 2014; 9:e89753. [PubMed: 24587012]
26. Tenney DJ, Levine SM, Rose RE, Walsh AW, Weinheimer SP, Discotto L, Plym M, Pokornowski K, Yu CF, Angus P, et al. Clinical emergence of entecavir-resistant hepatitis B virus requires additional substitutions in virus already resistant to Lamivudine. Antimicrob Agents Chemother. 2004; 48:3498–3507. [PubMed: 15328117]

27. Ciftci S, Keskin F, Cakiris A, Akyuz F, Pinarbasi B, Abaci N, Dincer E, Badur S, Kaymakoglu S, Ustek D. Analysis of potential antiviral resistance mutation profiles within the HBV reverse transcriptase in untreated chronic hepatitis B patients using an ultra-deep pyrosequencing method. Diagn Microbiol Infect Dis. 2014; 79:25–30. [PubMed: 24630522]
28. Colonno RJ, Rose R, Baldick CJ, Levine S, Pokornowski K, Yu CF, Walsh A, Fang J, Hsu M, Mazzucco C, et al. Entecavir resistance is rare in nucleoside naive patients with hepatitis B. Hepatology. 2006; 44:1656–1665. [PubMed: 17133475]
29. Tenney DJ, Rose RE, Baldick CJ, Levine SM, Pokornowski KA, Walsh AW, Fang J, Yu CF, Zhang S, Mazzucco CE, et al. Two-year assessment of entecavir resistance in Lamivudine-refractory hepatitis B virus patients reveals different clinical outcomes depending on the resistance substitutions present. Antimicrob Agents Chemother. 2007; 51:902–911. [PubMed: 17178796]
30. van Hemert FJ, Berkhout B, Zaaijer HL. Differential binding of tenofovir and adefovir to reverse transcriptase of hepatitis B virus. PLoS One. 2014; 9:e106324. [PubMed: 25180507]
31. Warner N, Locarnini S, Kuiper M, Bartholomeusz A, Ayres A, Yuen L, Shaw T. The L80I substitution in the reverse transcriptase domain of the hepatitis B virus polymerase is associated with lamivudine resistance and enhanced viral replication in vitro. Antimicrob Agents Chemother. 2007; 51:2285–2292. [PubMed: 17438047]
32. Quarleri J. Core promoter: a critical region where the hepatitis B virus makes decisions. World J Gastroenterol. 2014; 20:425–435. [PubMed: 24574711]
33. Glebe D, Urban S. Viral and cellular determinants involved in hepadnaviral entry. World J Gastroenterol. 2007; 13:22–38. [PubMed: 17206752]
34. Seeger C, Mason WS. Molecular biology of hepatitis B virus infection. Virology. 2015; 479–480:672–686.

Lay Summary

Long-term treatment with antiviral drugs carries the risk of selecting mutations in the hepatitis B virus (HBV). We herein report two cases of patients with insufficient response to dual tenofovir and entecavir therapy. Molecular analyses identified a distinct mutation, rtS78T/sC69*, that abolishes HBsAg detection, enhanced replication, sustained exosome-mediated virion secretion and decreased susceptibility to antivirals, thereby representing a potential high-risk mutation for HBV-infected individuals.

Highlights

- Two HBV-infected patients with incomplete viral suppression despite dual entecavir (ETV) and tenofovir (TDF) therapy carried the rtS78T/sC69* HBV mutation
- The rtS78T mutation causes enhanced viral replication and reduced susceptibility to ETV and TDF *in vitro*
- The sC69* mutation causes truncation of HBs protein without defective HBV secretion or intracellular HBsAg retention
- This mutation selected during ETV+TDF therapy may predispose to treatment failure and HBV-related carcinogenesis

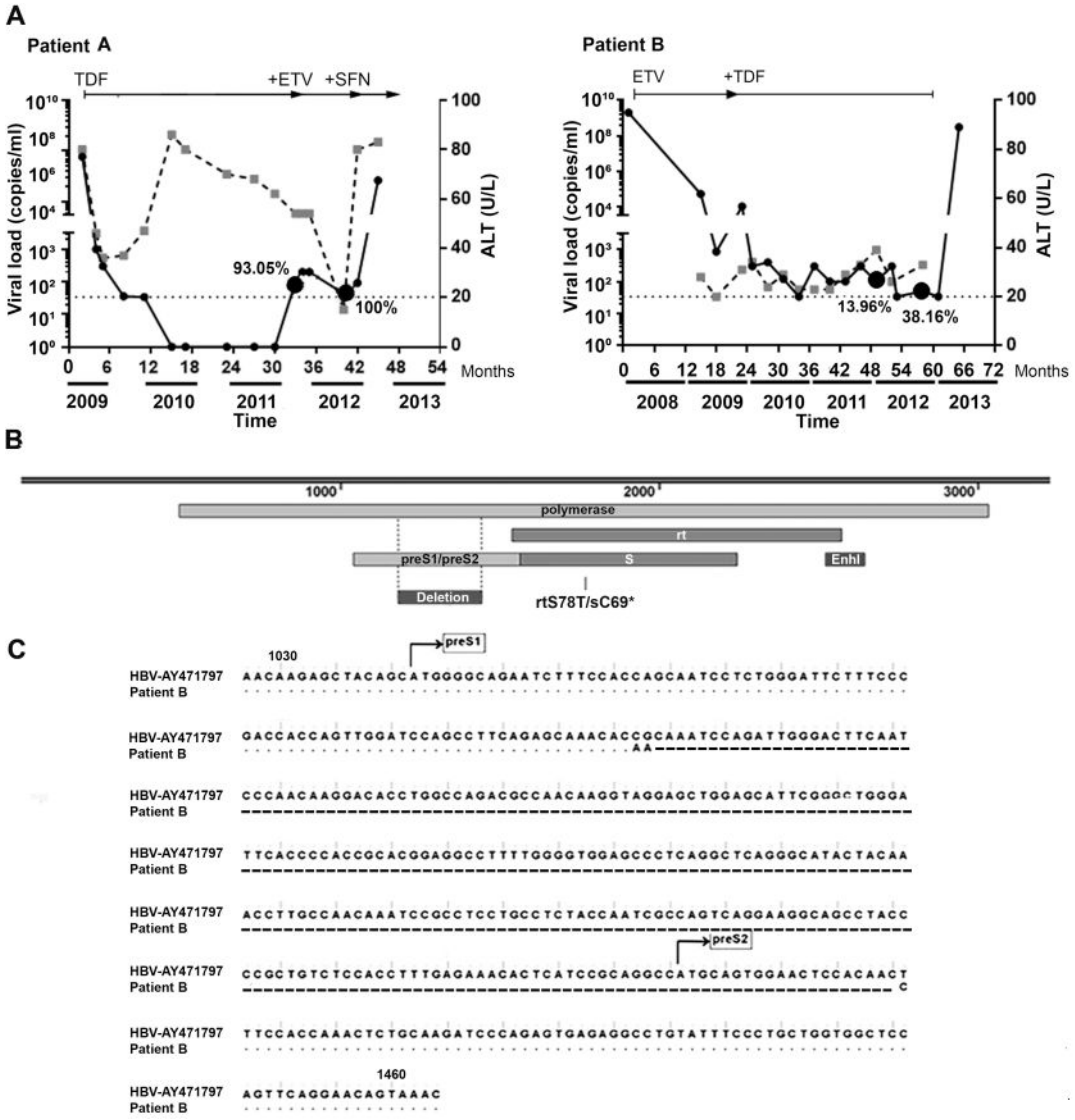

Figure 1. Clinical course of the patients

(A) HBV-DNA viral load (copies/ml, black line) and ALT levels (U/L, grey dashed line) in relation to antiviral treatment are shown for the two cases. Two sampling time points for sequencing analyses from each patient are highlighted by larger dark circles, and the corresponding frequency of rtS78T (%) is noted next to the circles. **(B)** Schematic representation of HBV polymerase, reverse transcriptase (rt), surface proteins (preS1/S2, S) and enhancer-I (EnhI) element, indicating the positioning of the rtS78T/sC69* mutation (M1 and M3) and the deletion preS1/S2del (M2 and M3). **(C)** The 261 base-pair in frame nucleotide deletion (nt 1124 to 1385) at the preS1/preS2 junction, which was detected through direct sequencing of HBV-DNA isolates from patient B at both time points, is shown by dashed line. Dots represent identical nucleotides at each position. *Abbreviations are:* ALT: alanine amino transferase activity, EnhI: Enhancer element I, ETV: entecavir, rt: reverse transcriptase gene, SFN: sorafenib, TDF: tenofovir, wt: wild type HBV.

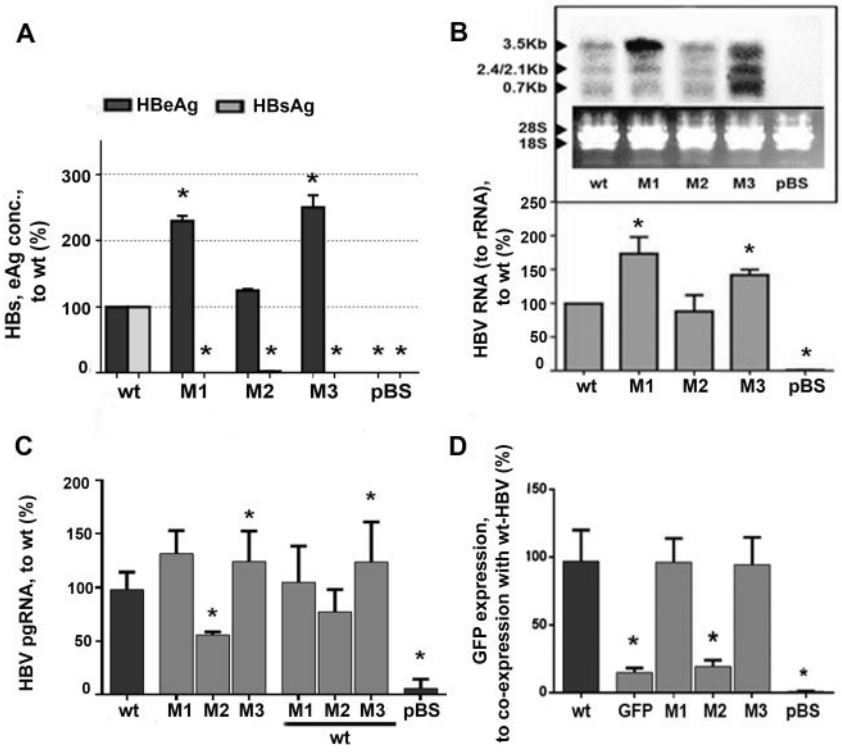

Figure 2. HBs and eAg expression and transcription efficacy of preS1/S2del, rtS78T/sC69* and pcDNA3.1(-)-eGFP constructs

(A) HBeAg (dark grey) and HBsAg (light grey) levels released from hepatoma cells transfected with wild type (wt) or mutant HBV constructs (M1, M2, and M3). (**B)** HBV-pgRNA levels were detected through Northern blot analysis of the RNAs probed with a full-length DIG-labeled HBV-DNA and normalized to ribosomal RNAs. **(C)** Single transfection of mutants and their co-transfection with wild type HBV (1:1 ratio), 3 days post transfection. pgRNA levels were defined through qPCR assay, and the results were normalized to relative GAPDH quantifications. Values are shown compared to wild type HBV. **(D)** Co-expression of pcDNA3.1(-)-eGFP (green fluorescent protein, GFP) and HBV. The concentration of GFP construct was kept the same across all the conditions. Values are represented compared to GFP co-expression with wild type HBV. M1: rtS78T/sC69*, M2: preS1/S2del, M3: rtS78T/sC69*+preS1/S2del, pBS: pBluescript (empty plasmid vector), pgRNA: pregenomic-RNA, wt: wild type HBV. *indicates p-value <0.05 (compared to wt).

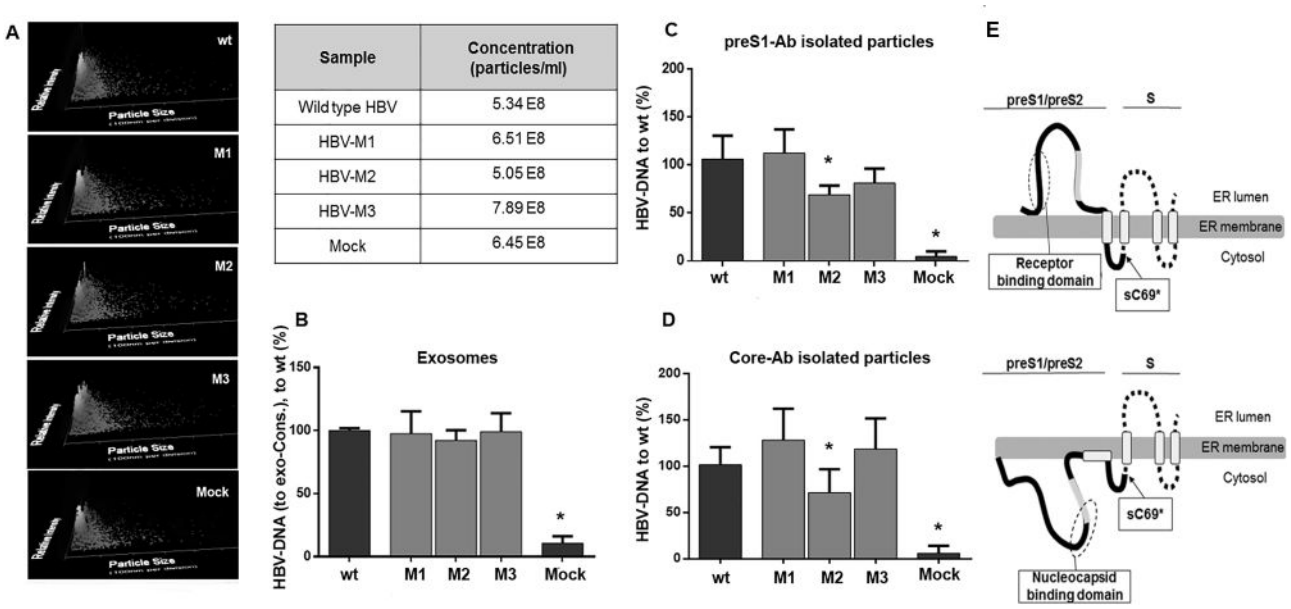

Figure 3. Alternative secretion of HBV particles

(A) Supernatant of transfected hepatoma cells was collected after 6 days of transfection, passed through 0.2μM filter and centrifuged two times at 110,000g for 70 minutes with one wash step in between. Pellets were analyzed for the quantity of their particles, with peaks at 37nm to 42nm (left panel). Particle concentrations are shown in the table. (**B)** Exosomes were isolated from the pellets and subjected to DNA extraction and qPCR analysis. Values are normalized to the particle concentrations and compared to the wild type HBV. (**C)** Supernatants collected during 6 days of transfection were isolated through overnight incubation with anti preS1-antibody and Protein A/G Plus-agarose precipitation. Extracted DNAs were quantified by qPCR assay. Values are shown compared to wild type HBV. **(D)** Naked nucleocapsids from collected supernatants were precipitated trough overnight incubation with anti-core antibody and Protein A/G Plus-agarose. After DNA extraction, samples were analyzed by qPCR. Values are shown compared to the wild type HBV transfections. **(E)** Schematic representation of sC69* mutation relative to preS1 (dark), preS2 (light) and S (dashed) protein. The external (above) and internal (below) orientations of preS1 are shown, and the domains involved in receptor and nucleocapsid binding are shown by dashed circles. *Abbreviations are:* Ab: antibody, Conc.: concentration, ER: endoplasmic reticulum, Exo.: exosomes, M1: rtS78T/sC69*, M2: preS1/S2del, M3: rtS78T/sC69*+preS1/S2del, wt: wild type HBV. *indicates p-value <0.05 (compared to wt).

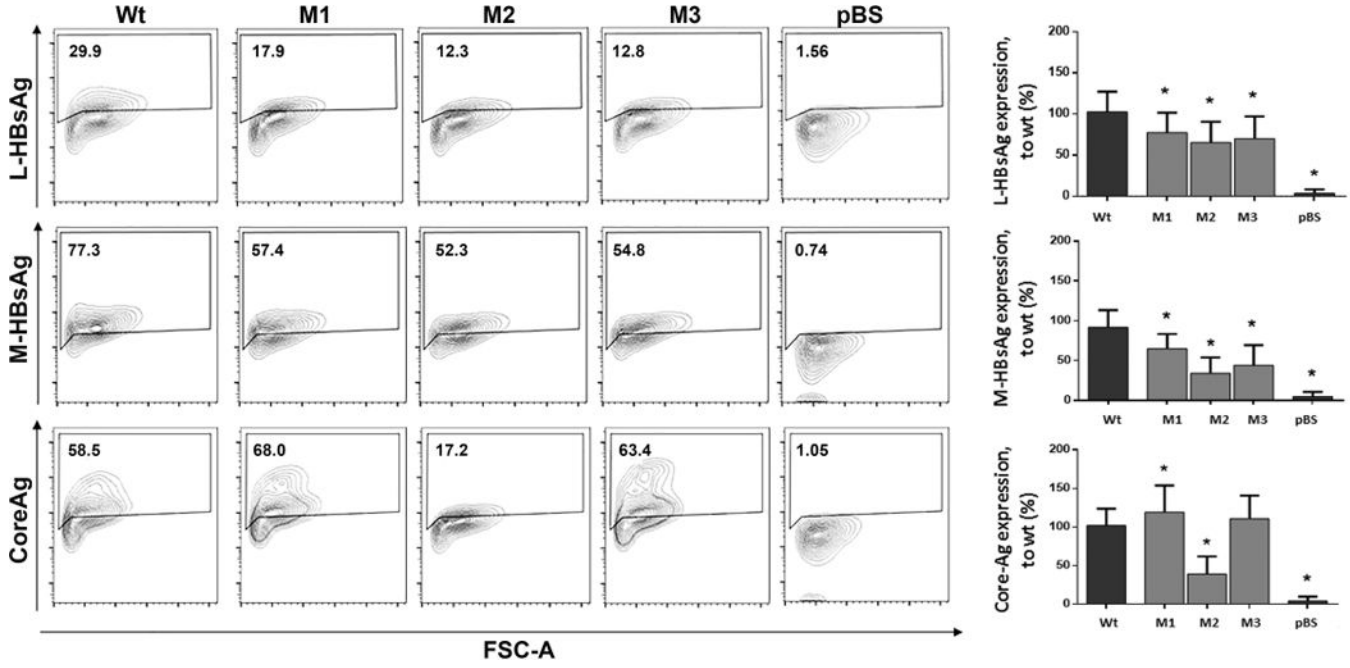

Figure 4. Expression analysis of intracellular HBV surface antigens and core protein due to rtS78T/sC69* and preS1/preS2del

Analysis of Huh7 cells for the expression of large (L)-HBsAg, medium (M)-HBsAg and Core-Antigen, 6 days post transfection. Collected cells were fixed with paraformaldehyde and incubated with anti-preS1 (upper row), anti-preS2 (middle row) and anti-core (lower row) antibodies and then stained with goat anti-mouse Alexa Fluor 647 as the secondary antibody. Representative FACS plots are shown, and the bar graphs summarize the findings compared to wild type HBV. *Abbreviations are:* Ag: antigen; L-HBsAg: large HBsAg, M-HBsAg: medium HBsAg, M1: rtS78T/sC69*, M2: preS1/S2del, M3: rtS78T/sC69*+preS1/S2del, pBS: pBluescript (empty plasmid vector, negative control), wt: wild type HBV. *indicates p-value <0.05 (compared to wt).

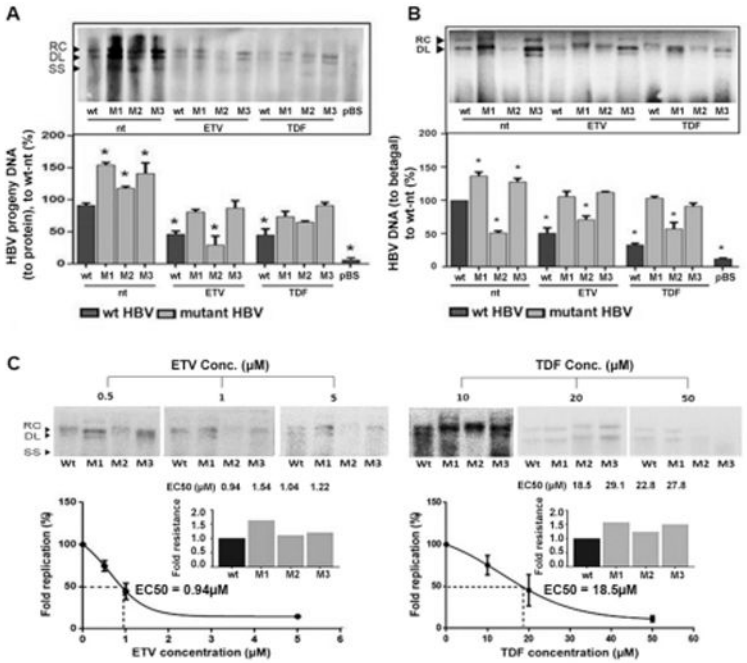

Figure 5. Influence of preS1/S2del and rtS78T/sC69* mutants on drug resistance *in vitro*

(A) HBV DNA structures by Southern blot (above) and HBV progeny DNA levels (below) in cells transfected with wild type (wt) or mutant constructs (M1, M2 and M3). The cells were either non-treated or treated with ETV (1μM) or TDF (20 μM). All values are presented relative to wt in no treatment (nt)-assay. **(B)** Extracellular HBV-DNA was extracted and quantified following polyethylene glycol isolation of secreted virions. Values are compared to the wt in nt-assay. ETV and TDF were used at 1μM and 20μM concentrations, respectively. Data were normalized to the transfection efficiency (controlled by beta-galactosidase measurement). **(C)** HBV DNA structures by Southern blot in three different concentrations of ETV and TDF (above panels). The half maximal effective concentrations (EC50) for ETV and TDF in treatment assays and the altered susceptibility of the mutant HBV isolates to the treatments is shown by fold resistance (below panels). *Abbreviations are:* DL: double stranded linear DNA, EC50: half maximal effective concentration, ETV: entecavir, M1: rtS78T/sC69*, M2: preS1/S2del, M3: rtS78T/sC69* +preS1/S2del, nt: no drug treatment, pBS: pBluescript (empty plasmid vector, negative control), RC: relaxed circular DNA, SS: single stranded DNA, TDF: tenofovir, wt: wild type HBV. *indicates p-value <0.05 (compared to wt).

Table 1

Frequency of mutations in HBV-reverse transcriptase (RT) and surface protein (HBsAg) of patients A and B, following ultra-deep pyrosequencing (UDPS) analysis of the HBV-genome at two time points for each patient.

variants			1st sampling	2nd sampling
RT	**Patient A**	**S78T**	**93.05**	**100**
		S6*_**S78T**	**0.50**	
		E10D_L4I_D7T_I16T_**S78T**	**0.70**	
		E10D_L4I_D7T_I16T	3.04	
		L101P	0.59	
	Patient B	E10D_L4I_D7T_I16T	74.24	32.14
		E10D_L4I_D7T_I16T_**S78T**	2.6	2.07
		I16T	0.33	
		S78T	**13.96**	**38.16**
		L77F_S78A		1.76
		H90N_I91L		0.24
		E10D_L4I_D7A_**S78T**		**2.07**
		I53N_S54Y_H90N_I91L		0.55
		E10D_L4I_D7A		0.52
		E10D_L4I_D7A_I53N_S54Y		0.53
		E10D_L4I_D7T_I16T_H90N_I91L		0.28
		E10D_L4I_D7A_I53N_S54Y_H90N_I91L		7.11
		E10D_L4I_D7T_I53N_S54Y_H90N_I91L		0.34
		T128N	0.71	1.65
		T128N_M204I	0.88	
		L180M		0.45
		L180M_M204V		1.37
		T128N_L180M		0.62
		T128N_L180M_M204V		2.98
		M204I	1.84	
		M204V		6.53
		A355E		3.39
HBsAg	**Patient A**	I68T_**C69***	**93.22**	**100**
		F8L_I68T_**C69***	**0.71**	
		G50D_I68T_**C69***	**0.23**	
		F8L	3.22	
		F93L	0.59	
	Patient B	F8L	74.06	32.58
		F8L_I68T_**C69***	**2.48**	**1.97**
		I68T_**C69***	**14.21**	**37.78**

variants			1st sampling	2nd sampling
		I68T_C69L		1.75
		I68T		0.65
		N3S_I68T_**C69***		**0.51**
		S45T_P46T_I68T		0.67
		N3S		0.54
		N3S_S45T_P46T_I68T		7.66
		F8L_S45T_P46T_I68T		0.40
		P120T_I195M		3.01
		P120T	0.71	2.29
		I195M		6.58
		P120T_W196S	0.86	
		W196S	1.87	